

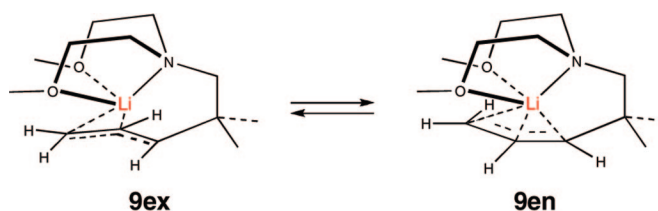
## Comparison of an Internally Coordinated 2-Pentenylithium with Its 4-Sila Analog. Structure and Dynamic Behavior: Unexpected $^{13}\text{C}/^7\text{Li}$ Spin Coupling

Gideon Fraenkel,<sup>\*,†</sup> José Cabral,<sup>‡</sup> Xiao Chen,<sup>†</sup> and Albert Chow<sup>†</sup>

Department of Chemistry, The Ohio State University, Columbus, Ohio 43210 and The Ohio State University, Newark Campus, Newark, Ohio 43055

fraenkel@mps.ohio-state.edu

Received October 6, 2008

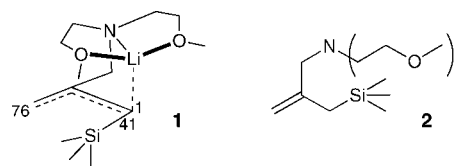


Four allylic lithium compounds have been prepared with a tethered ligand,  $(\text{CH}_3\text{OCH}_2\text{CH}_2)_2\text{NCH}_2\text{C}(\text{CH}_3)_2\text{-L}$ , attached to a terminal allyl carbon. They are equimolar equilibrium mixtures of 3-*endo-L*-allyllithium with 3-*exo-L*-allyllithium, **9en** and **9ex**, respectively, and (separately) 1-*exo-TMS*-3-*endo-L*-allyllithium with 1-*exo-TMS*-3-*exo-L*-allyllithium, **13en** and **13ex**, respectively. Carbon-13 NMR analysis shows that all four compounds are monomeric and internally coordinated, the allyl moiety in each one is partially localized, and  $^7\text{Li}$  is spin coupled to both  $^{31}\text{C}_1$  and  $^{13}\text{C}_2$  of allyl. NMR line shape changes show that **9en**, **9ex**, **13en**, and **13ex** all undergo fast transfer of the lithium-coordinated ligand between faces of the allyl planes at low temperatures. Within each equilibrium system the compound with the *exo*-tethered ligand inverts faster than its *endo* analog. All four compounds invert faster in  $\text{THF-}d_{10}$  compared to in diethyl ether- $d_{10}$  as solvent. Corresponding Eyring activation parameters are reported. Also, inversion in  $\text{THF-}d_8$  for all four compounds is characterized by large negative  $\Delta S^\ddagger$  values, whereas in diethyl ether- $d_{10}$   $\Delta S^\ddagger$  values for inversion are near neutral. NMR line shape changes due to the dynamics of bimolecular C,Li exchange and rotation around the  $\text{C}_2\text{-C}_3$  bonds are just detected via selective line broadening effects above 290 K. These processes are much slower than inversion.

### Introduction

The literature is replete with examples of directed reactions of organolithium compounds.<sup>1</sup> Typically in these reactions an organolithium compound complexes with a potential ligand on the substrate. The coordinated RLi compound then reacts with the substrate, usually by addition or by metalation. The initial product is an internally coordinated organolithium compound. What has not been generally acknowledged is that its electronic structure may differ from that of its externally solvated analog. This is especially true when the resulting carbanionic species is nominally delocalized. For example, a combination of NMR and X-ray crystallography established that the product **1** (shown

with terminal  $^{13}\text{C}$  shifts) of the metalation of **2** is partially localized.<sup>2</sup> There is even one bond scalar coupling between  $^6\text{Li}$



or  $^7\text{Li}$  with  $^{13}\text{C}$  of allyl, which is unheard of among delocalized lithium carbanide salts. We proposed that the ligand tether in **1** is too short to place  $\text{Li}^+$  normal to the center of the allyl plane

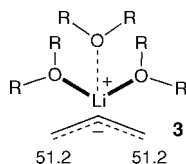
(1) Clayden, J. In *Organolithiums, Selectivity for Synthesis*; Pergamon: Amsterdam, 2006; Chapter 6, pp 273–337.

(2) (a) Fraenkel, G.; Qiu, F. *J. Am. Chem. Soc.* **1996**, *118*, 5828. (b) Fraenkel, G.; Qiu, F. *J. Am. Chem. Soc.* **1997**, *119*, 3571. (c) Fraenkel, G.; Liu, H.; Fleischer, R.; Chow, A. *J. Am. Chem. Soc.* **2004**, *126*, 3983.

<sup>†</sup> Columbus campus.

<sup>‡</sup> Newark campus.

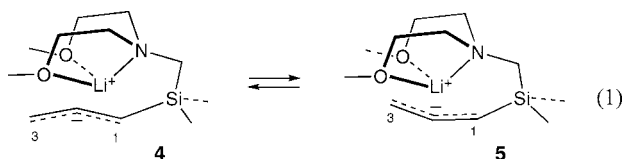
as in most externally coordinated allylic lithium compounds such as **3**<sup>3–5</sup> (shown with terminal allyl <sup>13</sup>C shifts). Instead Li<sup>+</sup> is placed normal to the allyl plane over one of the terminal carbons.



From this aberrant site Li<sup>+</sup> polarizes the allyl anion to become partially localized. We call this effect site specific electrostatic perturbation of conjugation, SSEPOC.<sup>6</sup> Compounds subject to SSEPOC are useful in organic synthesis. Because they are largely monomeric and carry their own solvation, they tend to react selectively. By contrast, externally solvated RLi compounds tend to assemble into rapidly interconverting mixtures of species that differ by solvation and aggregation and tend to react rapidly and indiscriminately.<sup>1</sup>

Effects due to SSEPOC tend to be continuous.<sup>2,6</sup> They depend on the nature of the nominally delocalized carbanion, the ligand, ligand tether, and substituents. Herein we report on the effect of changing the site of attachment of the ligand tether and how this new study has revealed some unexpected spin coupling interactions.

We previously reported that the silyl-substituted interconverting mixture of **4** and **5** (eq 1) was prepared in experiments to slow down exchange of ions between ion-pairs and thus facilitate NMR mapping studies of these ion-pairs.<sup>7</sup> NMR studies



confirmed that these compounds are indeed internally solvated and delocalized. Averaging effects observed among their NMR line shapes uncovered the dynamics of transfer of the coordinated ligand between faces of the allyl plane, as well as the interconversion between **4** and **5** by rotation around the C–CSi allyl bond.<sup>7</sup> Herein we report a study of the carbon analogs of **4** and **5**. Their structures and behavior are significantly different from those of **4** and **5**.

(3) (a) Koster, E.; Weiss, E. *Chem. Ber.* **1982**, *115*, 3422. (b) Schumann, U.; Weiss, E.; Dietrich, H.; Mahdi, W. *J. Organomet. Chem.* **1987**, *322*, 299. (c) Boche, G.; Etzrodt, H.; Marsh, M.; Massa, W.; Baum, G.; Dietrich, H.; Mahdi, W. *Angew. Chem.* **1986**, *98*, 84. (d) Boche, G.; Fraenkel, G.; Cabral, J.; Harris, K.; Eikema-Hommes, N. J. P. van; Lohrenz, J.; Marsch, M.; Schleyer, P. v. R. *J. Am. Chem. Soc.* **1992**, *114*, 4307. (e) Weiss, E. *Angew. Chem., Int. Ed. Engl.* **1993**, *32*, 1501.

(4) (a) Fraenkel, G.; Chow, A.; Winchester, W. R. *J. Am. Chem. Soc.* **1990**, *112*, 382. (b) Fraenkel, G.; Cabral, J.; Lanter, C.; Wang, J. *J. Org. Chem.* **1990**, *64*, 1302.

(5) (a) West, P.; Purmort, J. I.; McKinley, S. V. *J. Am. Chem. Soc.* **1968**, *90*, 797. (b) Thompson, T. B.; Ford, W. T. *J. Am. Chem. Soc.* **1979**, *101*, 5459. (c) Cabral, J.; Fraenkel, G. *J. Am. Chem. Soc.* **1992**, *114*, 9067. (d) Fraenkel, G.; Winchester, W. R. *J. Am. Chem. Soc.* **1989**, *111*, 3794. (e) Fraenkel, G.; Qiu, F. *J. Am. Chem. Soc.* **2000**, *122*, 12806. (f) Fraenkel, G.; Chow, A.; Winchester, W. R. *J. Am. Chem. Soc.* **1990**, *112*, 2582.

(6) (a) Fraenkel, G.; Duncan, J. H.; Wang, J. *J. Am. Chem. Soc.* **1999**, *121*, 432–443. (b) Fraenkel, G.; Fleischer, R.; Liu, H. *ARKIVOC* **2002**, *13*, 42–49. (c) Fraenkel, G.; Gallucci, J.; Liu, H. *J. Am. Chem. Soc.* **2006**, *128*, 8211. (d) Fraenkel, G.; Chen, X.; Gallucci, J.; Ren, Y. *J. Am. Chem. Soc.* **2008**, *130*, 4140–4145.

(7) Fraenkel, G.; Cabral, J. A. *J. Am. Chem. Soc.* **1993**, *115*, 1551–1557.

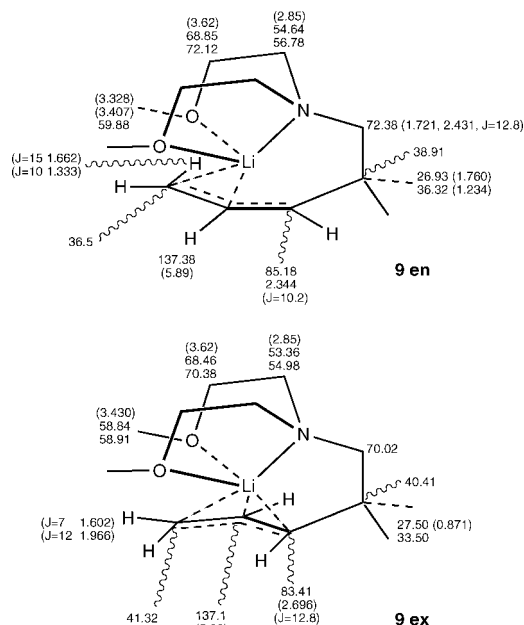
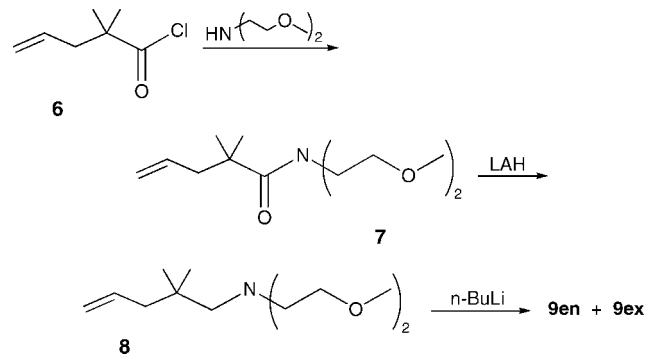


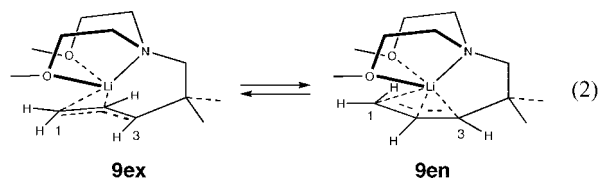
**FIGURE 1.** **9en** and **9ex** with <sup>13</sup>C and (<sup>1</sup>H) NMR shifts ( $\delta$  units) and vicinal proton coupling constants  $J$  (Hz) in diethyl ether-*d*<sub>10</sub> solution.

## Results and Discussion

Reactions **6** → **7** → **8** summarize the preparation of starting material **8**. Metalation of **8** with *n*-butyllithium in diethyl ether produced a 1:1 equilibrium mixture of the two isomeric internally coordinated allylic lithium compounds assigned as **9en** and **9ex**, respectively. Their proposed structures together



with associated NMR parameters are conveniently displayed in Figure 1 and eq 2. The stereochemistry of **9en** and **9ex** is readily assigned from their vicinal allyl proton coupling constants (see Figure 1).



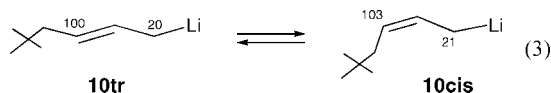
Further, inspection of the allyl methylene proton resonances of **9en** and **9ex** at 240 K shows that at this temperature rotation around their respective CH<sub>2</sub>–CH allyl bonds is slow relative to the NMR time scale.

The terminal allyl <sup>13</sup>C shifts of **9en** and **9ex** lie between those for a typical externally solvated delocalized allyllithium **3** and

**TABLE 1.** Coupling Constants  $^1J(^7\text{Li},^{13}\text{C})$  (Hz) of Internally Coordinated Allylic Lithium Compounds

	solvent			
	diethyl ether- $d_{10}$		THF- $d_8$	
	C <sub>1</sub>	C <sub>2</sub>	C <sub>1</sub>	C <sub>2</sub>
<b>9ex</b>	5.2	1.9		
<b>9en</b>	9.1	<1		
<b>13ex</b>	3.5	<1	<1	<1
<b>13en</b>	6.8	2.6	7.7	<1

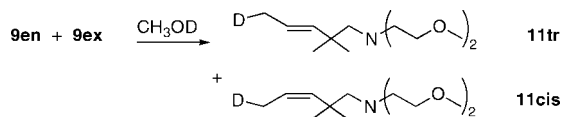
values for the unsolvated localized equilibrium mixture of **10tr** and **10cis**, which are drawn with their terminal  $^{13}\text{C}$  shifts.<sup>8</sup> The terminal allyl  $^{13}\text{C}$  shifts of **9en** and **9ex** resemble those for internally coordinated **1** and some similar compounds that were shown to be internally solvated and partially localized.<sup>2,6</sup>



Of the C<sub>1</sub> and C<sub>2</sub> allyl  $^{13}\text{C}$  resonances of **9en** and **9ex** at 230 K, all but C<sub>2</sub> of **9en** show quartet multiplicity due to one bond  $^{13}\text{C},^7\text{Li}$  scalar coupling; see Table 1. These assignments are confirmed by the results of a  $^7\text{Li}$  decoupling experiment, Figure 2. The  $^{13}\text{C}_2$  resonance of **9en**, which just consists of a broad line at 230 K, also narrows on decoupling  $^7\text{Li}$ . Altogether these results are consistent with monomeric structures for **9en** and **9ex**.

Observation of spin coupling between a central allyl  $^{13}\text{C}$  and  $^7\text{Li}$  in an allylic lithium compound is new with this study. However, broadening effects were observed previously in the  $^{13}\text{C}_2$  NMR of other internally solvated allylic lithium- $^7\text{Li}$  compounds.<sup>2,6</sup> These resonances sharpened both on warming the samples above 250 K and on cooling below this temperature. These effects are now consistent with  $^{13}\text{C},^7\text{Li}$  scalar coupling, which is progressively averaged both on warming due to increasing rates of bimolecular C,Li exchange and on cooling due to faster rates of  $^7\text{Li}$  nuclear electric quadrupole induced relaxation.<sup>9a</sup> Abragam has described the latter effect as “scalar relaxation of the second kind”.<sup>9b</sup> The expected fine structure due to  $^{13}\text{C},^7\text{Li}$  spin coupling is not observed because the rates of the two latter processes overlap. However, on the basis of the present study, these effects described above are clearly diagnostic of the operation of  $^{13}\text{C},^7\text{Li}$  scalar coupling.

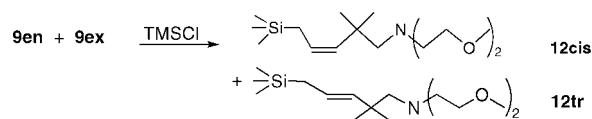
Deuterolysis of the **9en** and **9ex** mixture with methanol-OD produced a 1:1 mixture of the *cis* and *trans* 1-deuterio-2-alkenes **11cis** and **11tr**, which were identified by their NMR spectra.



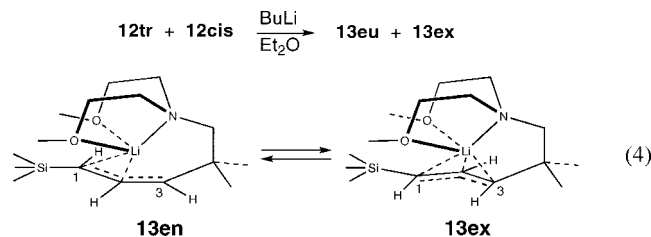
Solutions of **9en** with **9ex** in THF- $d_8$  exhibited NMR parameters similar to those obtained from the diethyl ether- $d_{10}$  solutions described above. However, inspection of the NMR spectra of these solutions revealed substantial contamination by the *trans* 1-deuterio-alkene **11tr**. The *cis* isomer **11cis** was not

detected in these spectra. Thus, the proton 1:1 doublet at 5.33  $\delta$  with 15.4 Hz separation observed in the contaminated sample of **9en** with **9ex** in THF- $d_8$  matches the same resonance in the proton NMR of the isolated mixture of **11cis** with **11tr** and is assigned to allyl C<sub>3</sub>H of **11tr** with a 15.4 Hz *trans* coupling to C<sub>2</sub>H. Further, of the four olefinic  $^{13}\text{C}$  resonances at 138.92, 122.99, 140.56 and 120.49 (all  $\delta$  units) observed in NMR of the above 1:1 mixture of **11tr** and **11cis**, only the last two resonances match shifts 120.06 and 141.03 observed in the contaminated sample of **9en** and **9ex** in THF- $d_8$ . The match is not identical because the product of dedeuteration of THF- $d_8$  is most likely complexed to **11tr**.

Treatment of the mixture of **9en** and **9ex** in ether with TMSCl gave a 1:1 mixture of the 1-silyl alkenes, **12cis** and **12tr**, identified by their NMR spectra. This mixture was metalated



with *n*-butyllithium in diethyl ether at  $-78^\circ\text{C}$ , yielding the equilibrium mixture **13en** and **13ex** (eq 4).



NMR samples of this mixture in diethyl ether- $d_{10}$  gave the  $^{13}\text{C}$  and  $^1\text{H}$  shifts and coupling constants listed around their proposed structures in Figure 3. Thus, the allyl vicinal proton coupling constants were used to assign the stereochemistry of the allyls, and then an HMQC experiment matched proton with  $^{13}\text{C}$  shifts for the two isomers. The terminal allyl  $^{13}\text{C}$  shifts resemble those previously assigned to partially localized allylic lithium compounds.<sup>2,6</sup>

Equal quartet splitting of  $^{13}\text{C}$  resonances of **13en** and **13ex** indicative of  $^{13}\text{C},^7\text{Li}$  spin coupling were observed for C<sub>1</sub> and C<sub>2</sub> of **13en** and C<sub>1</sub> of **13ex**, all in diethyl ether- $d_{10}$ , and for C<sub>1</sub> of **13en** in THF- $d_8$ ; see Table 1. This coupling was confirmed with a  $^7\text{Li}$  decoupling experiment for the diethyl ether- $d_{10}$  solution; see Figure 4. Where just broadening of the C<sub>1</sub> or C<sub>2</sub>  $^{13}\text{C}$  resonances was observed, these also sharpened on decoupling  $^7\text{Li}$ . The latter results also establish that **13en** and **13ex** are monomers.

Lithium proton HOESY proximity experiments  $^7\text{Li}\{^1\text{H}\}$  establish that whereas in **13en** there is only one strong  $^7\text{Li}$  interaction with the SiC<sub>1</sub>H proton and a weak one with protons on one methoxy group, in the case of **13ex** there are strong interactions between  $^7\text{Li}$  and the allyl protons on C<sub>1</sub>, C<sub>2</sub>, C<sub>3</sub>, and methoxy (Figure 5).

Changes of the  $^{13}\text{C}$  NMR line shapes of **9en** and **9ex** in diethyl ether- $d_{10}$  with temperature are indicative of several fast equilibrium molecular reorganization processes. For example, while the quaternary carbon resonances of (CH<sub>3</sub>)<sub>2</sub>C are both sharp up to 260 K, on warming above this temperature both undergo broadening. This is most likely due to slow interconversion between **9en** and **9ex** via rotation around the C<sub>2</sub>–C<sub>3</sub> bonds, Figure 6a. Also, on warming between 250 and 270 K, the  $^{13}\text{C}$

(8) (a) Fraenkel, G.; Halasa, A. F.; Mochel, V.; Stumpe, R.; Tate, D. *J. Org. Chem.* **1985**, *50*, 4563. (b) Glaze, W. H.; Jones, P. C. *J. Chem. Soc., Chem. Commun.* **1969**, 1434. (c) Glaze, W. H.; Hanicak, J. C.; Moore, M. L.; Chandhuri, J. J. *Organomet. Chem.* **1972**, *44*, 39. (d) Glaze, W. H.; Hanicak, J. E.; Chandhuri, J.; Moore, M. L.; Duncan, D. P. *J. Organomet. Chem.* **1973**, *51*, 13.

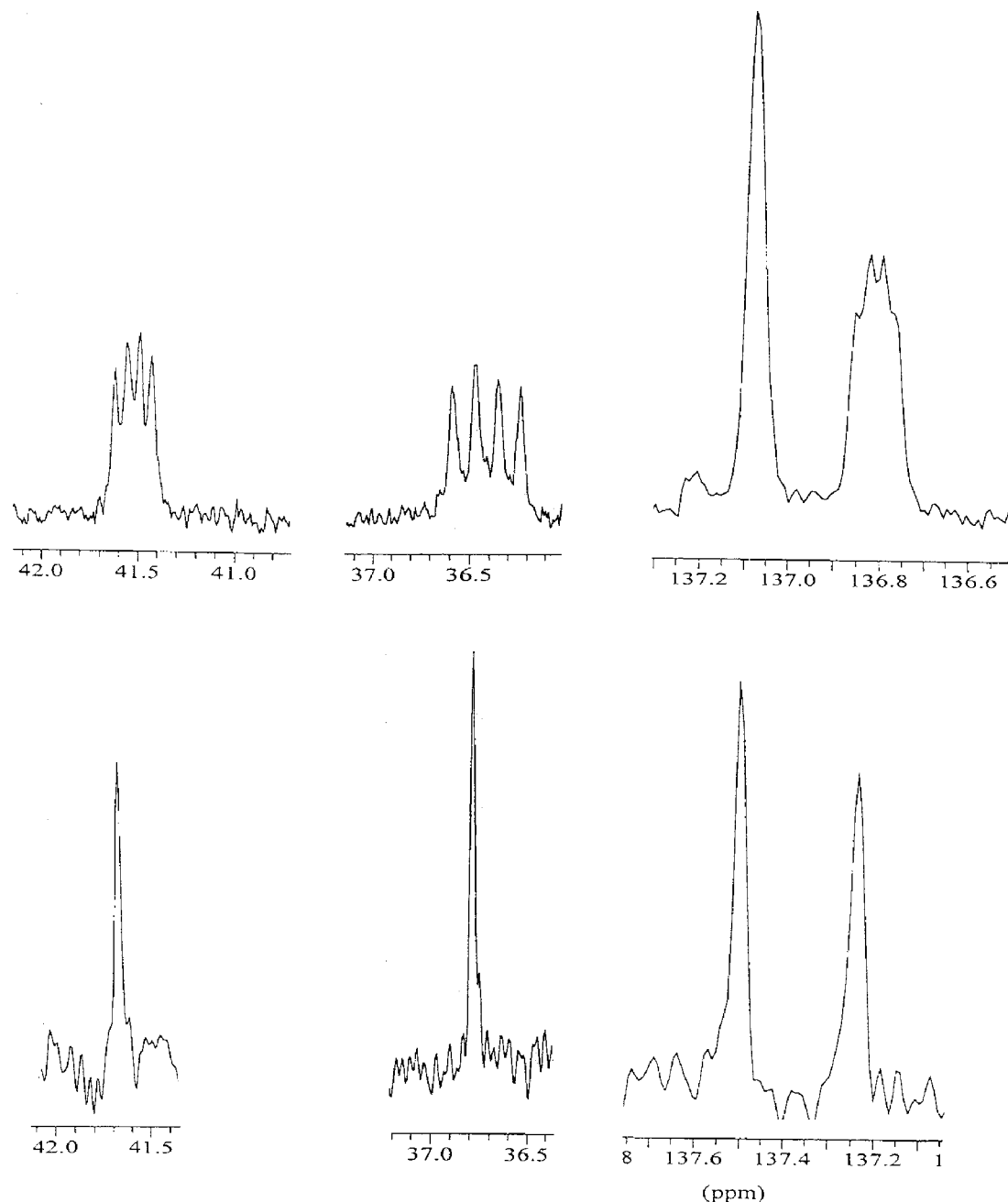


**FIGURE 2.** (Top)  $^{13}\text{C}$  NMR spectra ( $\delta$  units) of **9en** and **9ex**,  $\text{C}_1$  and  $\text{C}_2$  resonances in diethyl ether- $d_{10}$  solution at 240 K: left to right,  $\text{C}_1$  of **9ex**,  $\text{C}_1$  of **9en**,  $\text{C}_2$  of **9en** and  $\text{C}_2$  of **9ex**. (Bottom) Same order  $^7\text{Li}$  decoupled, 116.64 MHz.

quartets due to  $^{13}\text{C}, ^7\text{Li}$  coupling in **9ex** and **9en** undergo significant broadening. Such averaging of  $^{13}\text{C}, ^7\text{Li}$  coupling is clearly diagnostic of the onset of slow intermolecular C,Li bond exchange. Finally within a lower temperature range there is signal averaging due to fast transfer of coordinated lithium between faces of the allyl plane. Details are described as follows.

Taking into account all of the  $^{13}\text{C}$  NMR data for **9en** and **9ex** in diethyl ether- $d_{10}$  solution, it would appear that at a sufficiently low temperature the  $^{13}\text{C}$  resonances for geminal methyls,  $\text{OCH}_3$ ,  $\text{OCH}_2$ , and  $\text{NCH}_2\text{CH}_2$  would all consist of equal doublets for each compound. Given a sufficiently wide temperature range to observe the NMR spectra, with increasing temperature all of these doublets should progressively average to single lines at their respective centers. This behavior is observed for geminal methyls,  $\text{OCH}_2$ , and  $\text{NCH}_2\text{CH}_2$  of **9ex** and for  $\text{NCH}_2\text{CH}_2$  and  $\text{OCH}_3$  of **9en** both in

diethyl ether- $d_{10}$ . Other resonances exhibit only portions of these  $^{13}\text{C}$  line shape changes. These include the  $\text{OCH}_3$  resonance of **9ex**, which is a single broad line at 230 K and sharpens on warming. Also the sharp doublets observed for geminal methyls and  $\text{OCH}_2$  of **9en** just broaden with increasing temperature up to 290 K, Figure 6b.

Where practical, NMR line shape analysis has been carried out for these averaging  $^{13}\text{C}$  NMR doublets described above. They are treated as equally populated half-spin exchanging systems.<sup>10</sup> Derived Eyring activation parameters are listed in Table 2. As seen in Table 2, averaging of the geminal methyl

(9) (a) Fraenkel, G.; Subramanian, S.; Chow, A. *J. Am. Chem. Soc.* **1995**, *117*, 6300–6307. (b) Abragam, A. In *The Principles of Nuclear Magnetism*; Oxford University Press: London, 1961; pp 309–312.

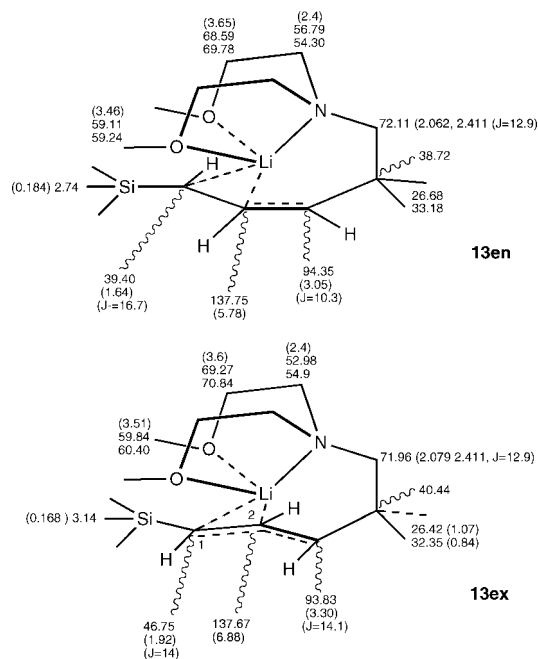


**FIGURE 3.** **13en** and **13ex** with  $^{13}\text{C}$  and  $^1\text{H}$  chemical shifts ( $\delta$  units) and vicinal proton coupling constants  $J$  (Hz) in diethyl ether- $d_{10}$  solution.

resonances of **9ex** gives rise to almost the same activation parameters as that due to the  $\text{NCH}_2\text{CH}_2$  resonances. Since averaging of the geminal methyl resonances is most likely due to transfer of the coordinated ligand between faces of the allyl, essentially inversion, then both sets of line shape changes are due to inversion. These results also establish that inversion at nitrogen accompanied by fast reversible dissociation of ligand lithium coordination must be a much slower process than face transfer of the coordinated ligand.

The dynamic behavior of **9en** in diethyl ether- $d_{10}$  solution behaves in a fashion similar to that of **9ex** with averaging of the ligand resonances of **9en** both reflecting the dynamics of face transfer of the coordinated ligand. Notice that of the two stereoisomers the  $\Delta H^\ddagger$  values are 4 kcal·mol larger for **9en** than for **9ex**. We would like to propose that lithium is more tightly bound in **9en** compared to **9ex** (Figure 6a and b).

In sum three reorganizational effects have been revealed, interconversion of **en** with **ex** isomers and bimolecular C,Li exchange, which are slow at higher temperatures of 270–300 K, and face transfer of coordinated ligand, which is fast at lower temperatures, 200–280 K.

Compounds **13en** and **13ex** undergo some  $^{13}\text{C}$  NMR line shape changes in a fashion similar to **9en** and **9ex**. In diethyl ether- $d_{10}$ , their  $^{13}\text{C}$  NMR quartets due to  $^{13}\text{C},^7\text{Li}$  coupling remain sharp and unchanged up to 300 K, indicating that intermolecular C,Li exchange is too slow to detect up to this temperature. In similar fashion interconversion of **13en** with **13ex** must be too slow to detect since the resonances due to the quaternary carbons of both species remain sharp and unchanged up to 300 K. Note that, as expected, throughout the temperature range studied the  $^7\text{Li}$  NMR remains a well resolved 1:1 doublet (Figure 8).

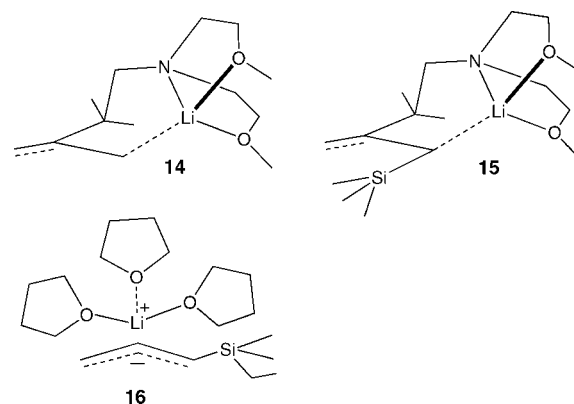
In contrast to the above results for diethyl ether- $d_{10}$  solutions, the two  $^{13}\text{C}$  quartet resonances due to  $\text{SiCH}$  of **13ex** and **13en**

in THF- $d_{10}$  broaden significantly on warming the sample above 260 K, which is indicative of slow intermolecular C,Li exchange. Note that intermolecular exchange is *not accompanied by interconversion of 13en with 13ex*, because throughout the temperature range studied the two  $^{13}\text{C}$  resonances due to the  $(\text{CH}_3)_2\text{C}$  quaternary carbons of **13en** and **13ex** remain sharp and unchanged as noted above.

Both stereoisomers **13en** and **13ex** exhibit NMR line shape changes reflective of the dynamics of inversion, Figure 9. Inversion is faster in **13ex** than in **13en** in both THF- $d_8$  and diethyl ether- $d_{10}$ . These effects are easily recognized by viewing the NMR line shapes. Thus, on warming the equilibrium mixture of **13en** with **13ex** in diethyl ether- $d_{10}$  solution between 230 and 290 K, the  $^{13}\text{C}$  line shapes due to geminal methyls,  $\text{CH}_3\text{O}$ ,  $\text{CH}_2\text{O}$ , and  $\text{NCH}_2\text{CH}_2$  of **13ex** all progressively change from separated doublets to averaged resonances at their respective centers. By contrast, the corresponding resonances due to **13en** all remain as sharp doublets, showing qualitatively that inversion in **13en** is the slower process compared to **13ex** (Figure 9). In similar fashion the  $^{13}\text{C}$  resonances due to geminal methyls,  $\text{CH}_2\text{O}$ ,  $\text{CH}_3\text{O}$ , and  $\text{NCH}_2\text{CH}_2$  of **13ex** in THF- $d_8$  solution are all averaged singlets by 230 K. However, by contrast, over the temperature range 230–290 K, the corresponding  $^{13}\text{C}$  resonances of **13en** (THF- $d_8$  solution) all exhibit the progressive changes from doublets to averaged resonances at their respective centers. Thus, due to experimental limitations of solubility at low temperatures and solvent boiling at the higher temperatures, it was possible only to undertake NMR line shape analysis of the above averaging doublets for resonances due to **13en** in THF- $d_8$  and those for **13ex** in diethyl ether- $d_{10}$ .

The results of these NMR line shape analyses are listed in Table 3.

Thus on the basis of the above account one can see qualitatively that in diethyl ether- $d_{10}$   $\Delta H^\ddagger$  for inversion of **13en** would be greater than 12.5 kcal·mol $^{-1}$ , whereas for **13ex** in THF- $d_8$  the  $\Delta H^\ddagger$  value for inversion would be less than 7 kcal·mol $^{-1}$ . In sum from the above dynamic data on **13en** and **13ex**, it appears that **13ex** inverts faster than **13en** in both THF- $d_8$  and diethyl ether- $d_{10}$ . Both **13en** and **13ex** invert faster in THF- $d_8$  compared to diethyl ether- $d_{10}$ . The inversion dynamics for **9en** and **9ex** in diethyl ether- $d_{10}$  follow the same pattern just described for **13en** and **13ex**. The data are summarized in Table 4.



Interactions that are already well-known to compromise conjugation include those due to steric effects, strain, and substituents. To these should now be added the electrostatic interactions that depend on the relative orientation of anion and

(10) (a) Kaplan, J. I.; Fraenkel, G. In *NMR of Chemically Exchanging Systems*; Academic Press: New York, 1980; Chapters 5 and 6. (b) Kaplan, J. I.; Fraenkel, G. *J. Am. Chem. Soc.* **1972**, *94*, 2907. (c) Gutowsky, H. S.; Saika, A. *J. Chem. Phys.* **1957**, *25*, 1288. (d) Kaplan, J. I. *J. Chem. Phys.* **1958**, *28*, 278.

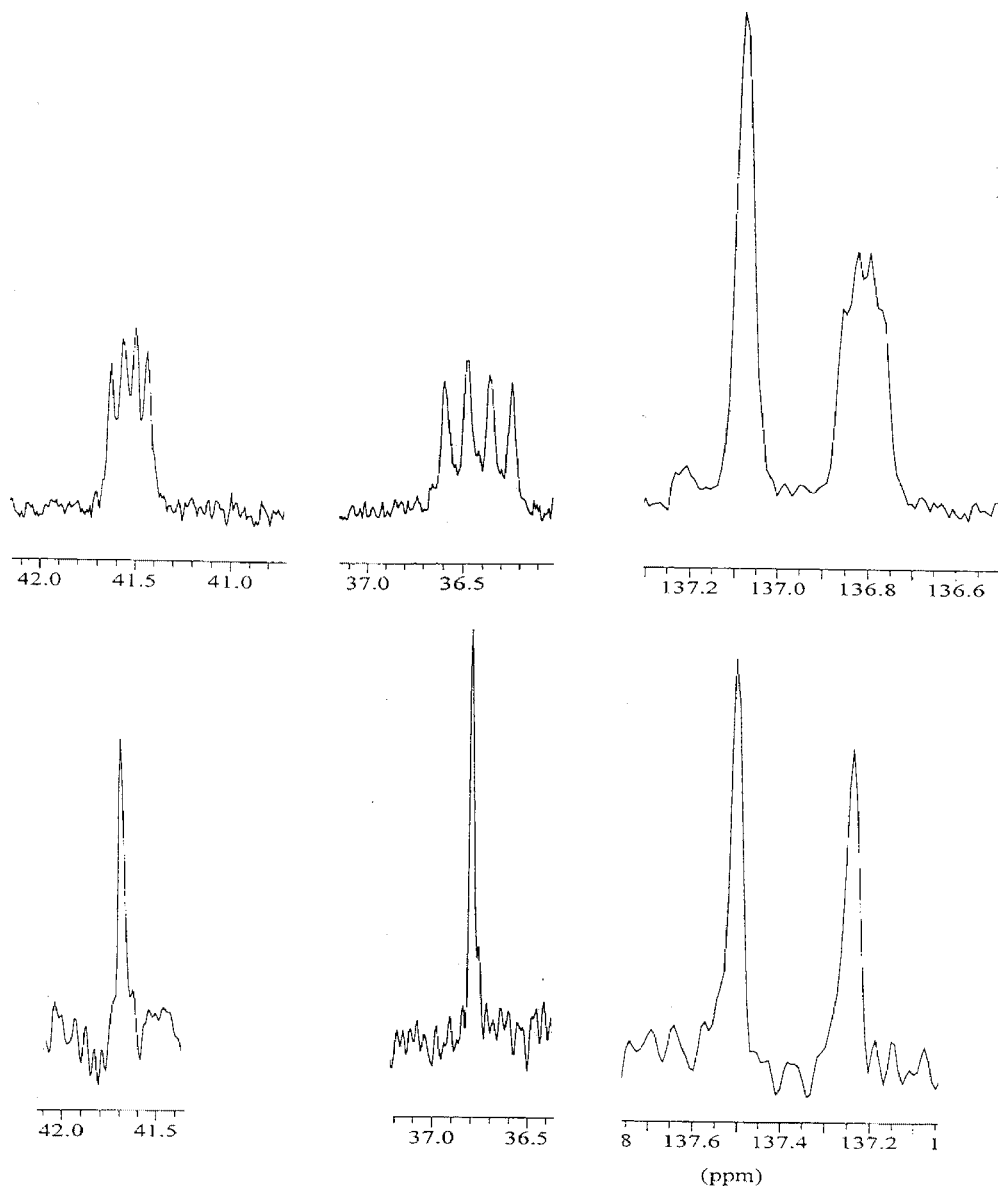


**FIGURE 4.** (Top)  $^{13}\text{C}$  NMR spectra ( $\delta$  units) of **13en** and **13ex**,  $\text{C}_1$  and  $\text{C}_2$  resonances in diethyl ether- $d_{10}$  solution at 240 K: left to right,  $\text{C}_1$  of **13ex**,  $\text{C}_1$  of **13en**,  $\text{C}_2$  of **13ex** and  $\text{C}_2$  of **13en**. (Bottom) Same order  $^7\text{Li}$  decoupled, 116.64 MHz.

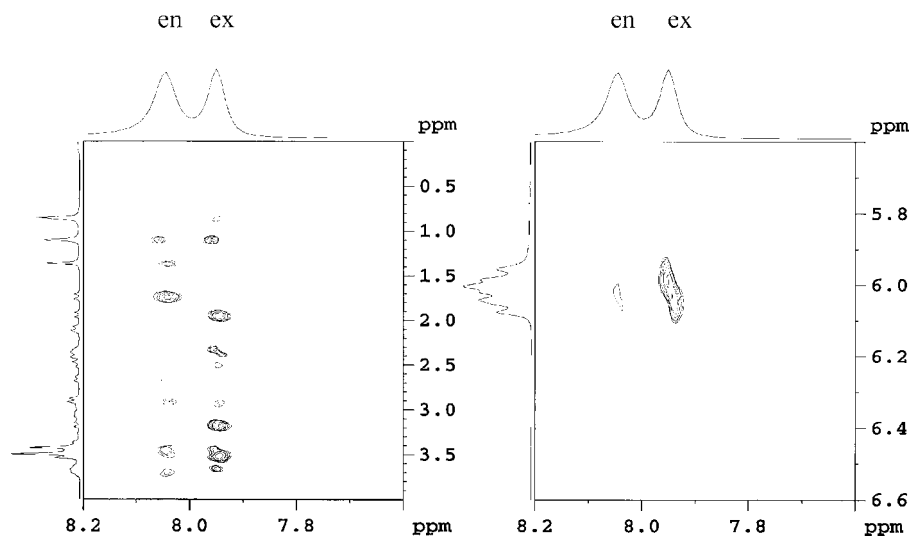


**FIGURE 5.**  $^7\text{Li}$   $\{^1\text{H}\}$  HOESY experiment, **13en** with **13ex** in diethyl ether- $d_{10}$  at 230 K. Axes: horizontal,  $^7\text{Li}$  shifts; vertical,  $^1\text{H}$  shifts.

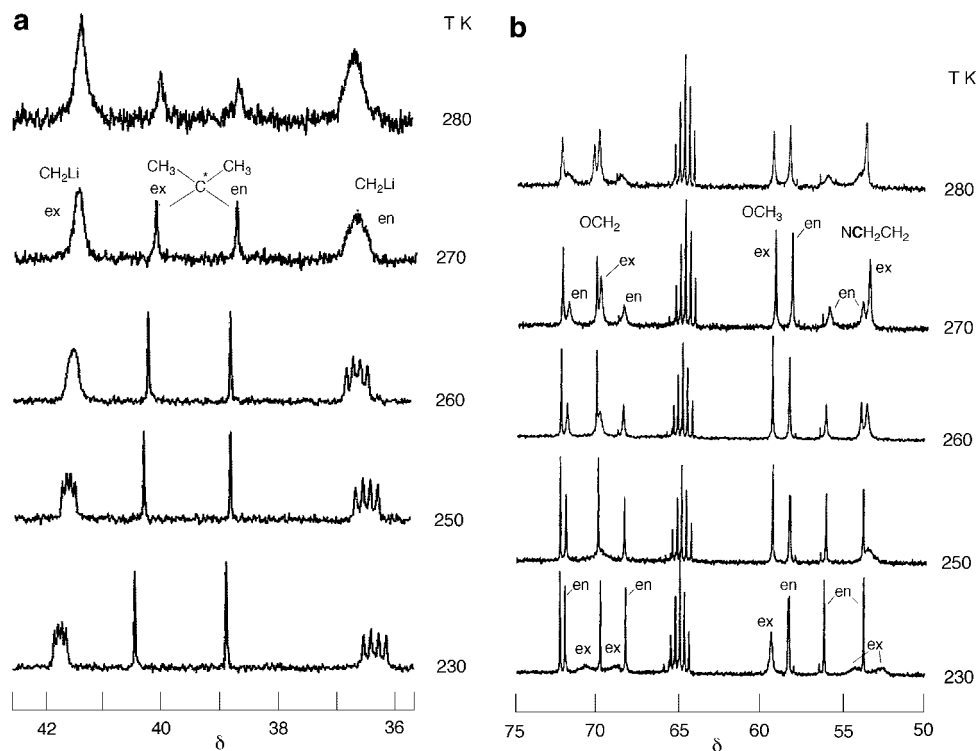


**FIGURE 6.** (a)  $^{13}\text{C}$  NMR spectra of **9en** and **9ex** in diethyl ether- $d_{10}$  solution, 38–44.5  $\delta$ , showing resonances for terminal  $\text{C}_1\text{H}_2$  allyl and  $(\text{CH}_3)_2\text{C}^*$  quaternary at different temperatures. (b)  $^{13}\text{C}$  NMR spectra of **9en** and **9ex** in diethyl ether- $d_{10}$  solution, 53–77  $\delta$ , at different temperatures, including  $\text{OCH}_2$ ,  $\text{OCH}_3$ , and  $\text{NCH}_2\text{CH}_2$  line shapes.

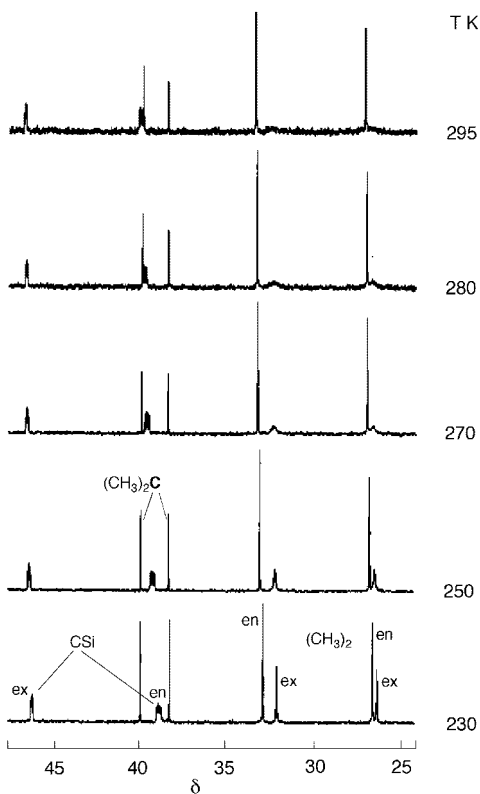


**FIGURE 7.**  $^{13}\text{C}$  NMR spectra of **13en** and **13ex** in diethyl ether- $d_{10}$  solution, 25–45  $\delta$ , at different temperatures.

cation within, for example, a set of internally coordinated allylic lithium compounds.<sup>2,6</sup> We found that the effect depends on the length of the ligand tether, nature of the ligand, and substituents

**TABLE 2.** Dynamics of Inversion of **9en** and **9ex** in Diethyl Ether- $d_{10}$

$^{13}\text{C}$ resonance	<b>9en</b>		<b>9ex</b>	
	$\Delta H^\ddagger$ (kcal·mol $^{-1}$ )	$\Delta S^\ddagger$ (eu)	$\Delta H^\ddagger$ (kcal·mol $^{-1}$ )	$\Delta S^\ddagger$ (eu)
$\text{NCH}_2\text{CH}_2$	$13.6 \pm 1$	$-0.7 \pm 0.3$	$9.8 \pm 1$	$-6 \pm 2$
$\text{OCH}_2$	$13.7 \pm 1$	$-0.2 \pm 0.1$		
$\text{C}(\text{CH}_3)_2$			$9.7 \pm 1$	$-6 \pm 2$

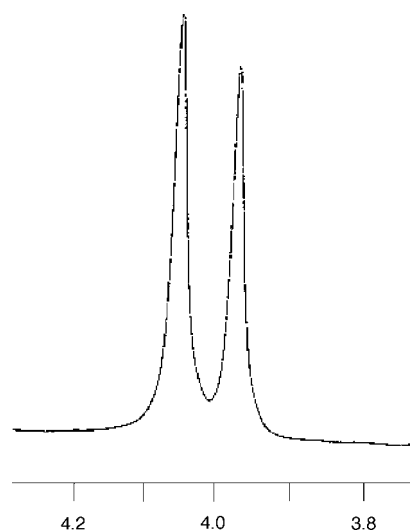


**FIGURE 8.**  $^7\text{Li}$  NMR spectrum of **13en** and **13ex** in diethyl ether- $d_{10}$  solution at 290 K, 116.64 MHz.

on allyl. In the current study the ligand has been attached to a terminal carbon of allylic lithium compounds defined collectively as **T-3**. Comparing the latter set, **9en**, **9ex**, **13en**, and **13ex**, with previously investigated analogs with the ligand tether

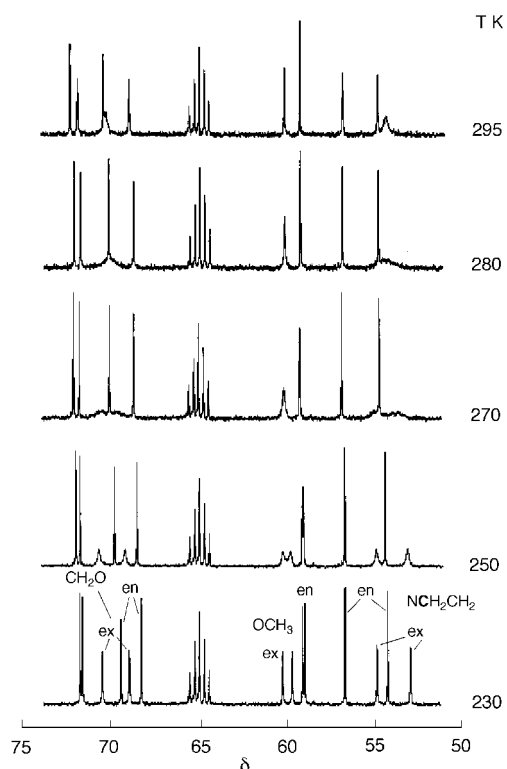


**FIGURE 9.**  $^{13}\text{C}$  NMR spectra of **13en** and **13ex** in diethyl ether- $d_{10}$  solution, 50–55  $\delta$ , at different temperatures.

**TABLE 3.** Dynamics of Inversion of **13en** in THF- $d_8$  and **13ex** in Diethyl Ether- $d_{10}$

$^{13}\text{C}$ resonance	<b>13en</b> , THF		<b>13ex</b> , diethyl ether- $d_{10}$	
	$\Delta H^\ddagger$ (kcal·mol $^{-1}$ )	$\Delta S^\ddagger$ (eu)	$\Delta H^\ddagger$ (kcal·mol $^{-1}$ )	$\Delta S^\ddagger$ (eu)
C(CH $_3$ ) $_2$	7.0 $\pm$ 0.7	-20 $\pm$ 3		
CH $_2$ O	6.7 $\pm$ 0.7	-21 $\pm$ 3	12.7 $\pm$ 1.2	-0.4 $\pm$ 0.3
CH $_2$ CH $_2$ N	7.6 $\pm$ 0.7	-17 $\pm$ 2.5	12.3 $\pm$ 1.2	-2 $\pm$ 1
CH $_3$ O			12.4 $\pm$ 1.2	-1.4 $\pm$ 1

**TABLE 4.** Allylic Lithium Compounds, Allyl  $^{13}\text{C}$  shifts,  $\delta$  Scale, and Dynamic Parameters for Inversion<sup>a</sup>

compd, solv	$\delta_1$	$\delta_2$	$\delta_3$	$\Delta H^\ddagger$ (kcal·mol $^{-1}$ )	$\Delta S^\ddagger$ (eu)
<b>4</b> , <sup>b</sup> THF- $d_8$	45.09	146.61	74.48	7.5	-15
<b>5</b> , <sup>b</sup> THF- $d_8$	45.09	148.12	74.50	7	-15
<b>9ex</b> , Et $_2$ O- $d_{10}$	43.12	137.10	83.49	9.8 <sup>c</sup>	-6 <sup>c</sup>
<b>9en</b> , Et $_2$ O- $d_{10}$	36.50	137.38	85.12	13.7 <sup>c</sup>	-0.5 <sup>c</sup>
<b>13en</b> , Et $_2$ O- $d_{10}$	39.40	137.75	94.35	>12.5	
<b>13en</b> , THF- $d_8$	41.40	137.80	94.20	7.1 <sup>c</sup>	-19 <sup>c</sup>
<b>13ex</b> , Et $_2$ O- $d_{10}$	46.75	137.67	93.83	12.5 <sup>c</sup>	-1
<b>13ex</b> , THF- $d_8$	46.90	138.00	93.81	<7.1	
<b>14</b> , <sup>d</sup> Et $_2$ O- $d_{10}$	51.62 <sup>e</sup>	165.90	51.62 <sup>e</sup>		
<b>15</b> , <sup>f</sup> Et $_2$ O- $d_{10}$	37.50	136.34	72.52	15	2
<b>16</b> , <sup>g</sup> TMEDA in Et $_2$ O- $d_{10}$	53.03	149.12	64.31	4.9	-21

<sup>a</sup> For numbering see structures in text. <sup>b</sup> Reference 7. <sup>c</sup> Activation parameters are average of all line shape sets; see Tables 2 and 3. <sup>d</sup> Reference 2c. <sup>e</sup> Averaged by a fast sigmatropic shift. <sup>f</sup> Reference 6a. <sup>g</sup> Reference 4a.

attached to the central allyl carbon in **1**, we see that all are internally coordinated and almost all are monomeric. Most of these compounds display  $^6\text{Li}$  or  $^7\text{Li}$  spin coupling to a terminal allyl  $^{13}\text{C}$ . However, the group with ligand attached to the terminal allyl carbon (called **T-3**) also exhibit  $^7\text{Li}$  coupling to  $^{13}\text{C}_2$  of the allyl. Previously the absence of these lithium allyl

$^{13}\text{C}_2$  couplings has been ascribed to averaging due to fast intermolecular C,Li exchange.<sup>2,6</sup>

As of the date of this writing, lithium allyl  $^{13}\text{C}$  spin coupling has not been reported for any externally solvated allylic lithium compound. The origin of such coupling within internally coordinated allylic lithium compounds has not yet been discussed. However, note that X-ray crystallography of **1** revealed separations between lithium and allyl carbons C $_1$ , C $_2$ , and C $_3$  of 2.125 Å, 2.640 Å and 3.691 Å, respectively.<sup>2c</sup> We have also undertaken some preliminary B3LYP/G-611G\* calculations<sup>2c</sup> to model **9en** and **9ex**. These have revealed lithium C $_1$ , C $_2$ , and C $_3$  allyl carbon separations of, respectively, 2.137, 2.314, and 2.694 Å for **9en** and in the same order 2.283, 2.340, and 2.356 Å for **9ex**. Since  $^7\text{Li}$  couples to only  $^{13}\text{C}_1$  of **1** but to  $^{13}\text{C}_1$  and  $^{13}\text{C}_2$  of **9en** and **9ex**, it would appear that lithium carbon proximity favors  $^7\text{Li}$   $^{13}\text{C}$  spin coupling.

It is now instructive to compare the structures and dynamic behavior of **9ex** and **9en** with their 4-sila analogs **47** and **5**,<sup>7</sup> respectively, and of the first two with analog **14**, which differs from **9en** and **9ex** in the site of attachment of the ligand tether; dynamic and  $^{13}\text{C}$  shift data are summarized in Table 4.

Previous X-ray crystallographic<sup>3</sup> and  $^{13}\text{C}$  NMR studies<sup>4,5</sup> of allylic lithium have established that as the  $^{13}\text{C}$  chemical shifts of the terminal allyl carbons change from identical or almost identical, as in externally solvated allyllithium **3**, to resembling those of a simple alkene, as in unsolvated **10tr** and **10cis**, there is a continuous change from delocalized in **3** to localized in **10tr** and **10cis**.<sup>2,6</sup>

From their allyl  $^{13}\text{C}$  chemical shifts one can see that **9ex** and **9en** are considerably localized when compared to allyl  $^{13}\text{C}$  shifts in **4** and **5**. A larger C $_2$ –C $_3$   $\pi$  bond order in **9en** and **9ex**, due to the carbon substituent at C $_3$ , compared to the C $_1$ –C $_2$  bond in **4** and **5** would be consistent with slower rotation around the C $_2$ –C $_3$  allyl bond in **9en** and **9ex**,  $k_1 = 2 \text{ s}^{-1}$  at 290 K compared to  $1000 \text{ s}^{-1}$  for the corresponding rotation that interconverts **4** and **5**.<sup>7</sup> In addition **9en** and **9ex** exhibit spin coupling between  $^7\text{Li}$  and both  $^{13}\text{C}_1$  and  $^{13}\text{C}_2$  of allyl. Such spin coupling was not observed among NMR data for **4** and **5**.

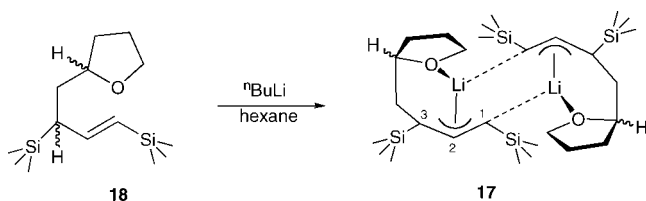
Compound **14** is the analog of **9en** and **9ex** with the ligand tether attached to the central allyl carbon. X-ray crystallography established an internally coordinated partially localized structure for **14** with allyl bond lengths of 1.366 Å for C $_2$ –C $_3$  and 1.426 Å for C $_1$ –C $_2$ .<sup>2c</sup> However, the  $^{13}\text{C}$  NMR of the terminal allyl carbons of **14** in diethyl ether- $d_{10}$  solution at 290 K consisted of a single sharp line due to a fast 1,3 lithium sigmatropic shift. This was evidenced by a broadening of this resonance with decreasing temperature; it finally disappeared into the baseline by 170 K. However, using the terminal allyl  $^{13}\text{C}$  line width at 250 K in conjunction with a calculated value for the  $\delta_1$ – $\delta_3$  shift difference obtained via DFT calculations, we estimated  $k_1$  for the sigmatropic shift to be  $1.4 \times 10^5 \text{ s}^{-1}$ .<sup>2c</sup> Since this fast sigmatropic shift also brings about inversion, it was not possible to resolve the dynamics of face transfer of coordinated lithium from that of the sigmatropic shift.

In a fashion similar to the relationships among **9en**, **9ex**, and **14**, compounds **13en**, **13ex**, and **15** share most common structural features with the exception that the ligand tether in **15** is attached at C $_2$  compared to C $_3$  in **13en** and **13ex**. All three compounds are internally coordinated. All exhibit spin coupling between  $^7\text{Li}$  and  $^{13}\text{C}_1$ , while in **13en** and **13ex**  $^7\text{Li}$  also couples to  $^{13}\text{C}_2$ . Inspection of the  $^{13}\text{C}$  shifts reveals that starting with recognized  $\pi$ -delocalized **16**, localization increases in the order **15**, then **13en** and **13ex**, similar (Table 4).



It is interesting that in a common solvent, diethyl ether- $d_{10}$ , inversion rates are quite similar for **9en**, **13ex**, and **15** despite different substitution and different sites of attachment of the ligand tether to the allyl moiety. Further, taking all of the inversion data together, in a common solvent we see that the *exo* isomer of a pair inverts faster than the *endo* isomer and each compound reported inverts faster in THF- $d_8$  compared to diethyl ether- $d_{10}$  as solvent. In cases where it has been practical to measure the activation parameters in THF- $d_8$ ,  $\Delta H^\ddagger$  for inversion is typically 7 kcal·mol<sup>-1</sup> with  $\Delta S^\ddagger$  large and negative, whereas in diethyl ether- $d_{10}$   $\Delta H^\ddagger$  is 10–13.5 kcal·mol<sup>-1</sup> with  $\Delta S^\ddagger$  close to neutral. Evidently in THF- $d_8$  development of the transition structure for inversion is accompanied by an increase in solvation, which is not the case for the process in diethyl ether- $d_{10}$ . Clearly the inversion mechanisms are different in the two solvents. Among compounds **9en**, **9ex**, **13en**, and **13ex** with ligand tether at the terminal allyl carbon (**T-3** group), the rates of bimolecular C,Li bond exchange are slow or too slow to measure. By contrast, in the case of most internally solvated allylic lithium compounds with the ligand tether attached to the central allylic carbon (**T-2** group),  $\Delta H^\ddagger$  for this process is within the range 11.5 ± 0.5 kcal·mol<sup>-1</sup>. We would like to propose that this effect is due to stronger electrostatic interaction between lithium and the allyl moiety in the **T-3** group compared to the **T-2** group.

In parallel to our results described above, a recent X-ray crystallographic study of the product **17** of metalation of **18** by *n*-butyllithium revealed internal coordination of Li<sup>+</sup> and partial localization within a dimeric structure.<sup>11</sup> Allyl bond lengths reported are C<sub>1</sub>–C<sub>2</sub> = 1.431 Å and C<sub>2</sub>–C<sub>3</sub> = 1.376 Å, similar to results for several internally coordinated allylic lithium compounds described by us previously.<sup>2,6</sup> In addition lithium is closer to the terminal and center allyl carbons, 2.313 and 2.194 Å, respectively, than to C<sub>3</sub>, 2.489 Å.



In sum, while externally solvated allyllithium with Li<sup>+</sup> normal to the center of the allyl plane is regarded to be fully delocalized when allyllithium is internally coordinated to a pendant ligand tethered at the allyl terminus C<sub>3</sub> or the allyl center C<sub>2</sub>,<sup>2,6</sup> conjugation is seriously compromised. In these cases the ligand places Li<sup>+</sup> normal to the allyl plane near C<sub>1</sub>. From this site Li<sup>+</sup> polarizes all to be partially localized. Among the four compounds reported herein allyl localization is enhanced by the alkyl tether at C<sub>3</sub>, which stabilizes  $\pi$  structure of the C<sub>2</sub>–C<sub>3</sub> bond, and by Si at C<sub>1</sub>, which stabilizes carbanionic character at C<sub>1</sub>. Comparing the equilibrium dynamic behavior of the C<sub>2</sub>-<sup>2,6</sup> versus the C<sub>3</sub>-ligand tethered compounds, we note that intermolecular C,Li exchange and inversion are both slower for the latter compounds due to their stronger Li<sup>+</sup> allyl electrostatic attraction.

## Experimental Section

**2,2-Dimethyl-4-pentenoyl Chloride (6).** A solution of 2,2-dimethyl-4-pentenoic acid (15.82 g, 0.123 mol) dissolved in 25 mL of diethyl ether was added dropwise from an addition funnel to thionyl chloride (19.5 g, 0.145 mol) at room temperature into a

100-mL Schlenk flask, with stirring, under an atmosphere of argon. Stirring continued after the above addition for 2 h at room temperature. Ether was distilled out at atmospheric pressure. The residue was distilled at 85 °C/80 Torr giving 16.11 g of the title product in 89.1% yield. <sup>13</sup>C NMR (CDCl<sub>3</sub>, 62.9 MHz,  $\delta$ ): 179.4, 132.24, 119.4, 52.6, 44.17. <sup>1</sup>H NMR (CDCl<sub>3</sub>, 250 MHz,  $\delta$ ): 1.260 (s, 6), 2.363 (2, d, *J* = 9.2 Hz), 5.069 (1, m), 5.137 (1, m), 5.688 (1, m).

**2,2-Dimethyl-*N,N*-bis(2-methoxyethyl)-4-pentenoamide (7).** Under a flow of argon, a solution of 2,2-dimethyl-4-pentenoyl chloride<sup>12</sup> (5.32 g, 0.032 mol) dissolved in 50 mL of diethyl ether was added dropwise from an addition funnel to bis(2-methoxyethyl)-amine (10.9 g, 0.0819 mol) in 50 mL of diethyl ether at room temperature in a 250-mL round-bottom flask. After addition the mixture was stirred for 6 h at room temperature. Following gravity filtration the precipitate was washed three times, each with 20 mL of diethyl ether. The combined ether extracts were washed with saturated Na<sub>2</sub>CO<sub>3</sub> and dried over MgSO<sub>4</sub>, and ether was removed by rotary evaporation. Vacuum distillation of the residue at 92 °C/4 Torr gave 8.6 g of the title product in 97% yield. <sup>13</sup>C NMR (CDCl<sub>3</sub>, 62.9 MHz,  $\delta$ ): 176.53, 134.55, 117.42, 70.84, 58.76, 48.09, 45.24, 42.38. <sup>1</sup>H NMR (CDCl<sub>3</sub>, 250 MHz,  $\delta$ ): 1.186 (6, s), 2.292 (2, d, *J* = 7.25 Hz), 3.42 (6, s), 3.44 (4, t, *J* = 5.4 Hz), 3.55 (4, b), 4.947 (1, d), 5.000 (1 s, b), 5.667 (1, m).

**5-Bis(2-methoxyethyl)amino-4,4-dimethyl-1-pentene (8).** A solution of 2,2-dimethyl-1-*N,N*-bis(2-methoxyethyl)-4-pentenoamide (5.13 g, 0.0268 mol) in 25 mL of THF was added dropwise to LAH (3.73 g, 0.08 mol) in 100 mL of THF at 0 °C. After this addition, the reaction mixture was allowed to come to room temperature with stirring over 4 h. The mixture was then quenched by slow addition of ice chips, and the nonaqueous phase was extracted with saturated NH<sub>4</sub>Cl. The organic phase was dried over MgSO<sub>4</sub>, and solvent was removed by rotary evaporation. Vacuum distillation of the residue, bp 75 °C/3.8 Torr, gave 4.74 g of the title product. <sup>13</sup>C NMR (CDCl<sub>3</sub>, 62.9 MHz,  $\delta$ ): 135.79, 116.67, 71.48, 67.57, 58.78, 56.51, 45, 35.92, 25.22. <sup>1</sup>H NMR (CDCl<sub>3</sub>, 250 MHz,  $\delta$ ): 0.789 (6, s), 1.915 (2, d, *J* = 7.4 Hz), 2.263 (2, s), 2.269 (4, t, *J* = 6.5 Hz), 3.288 (6, s), 3.403 (4, t, *J* = 6.5 Hz), 4.926 (1, d), 4.938 (1, b), 5.760 (1, m).

**3-*exo*- and 3-*endo*-5[Bis(2-Methoxyethyl)amino]-4,4-dimethyl-2-pentene-1-yl Lithium (9en and 9ex).** A 25-mL Schlenk tube was charged with 4 mL of dry diethyl ether and amine **8** (688.1 mg, 3 mmol) under an argon flow. *n*-Butyllithium (1.88 mL, 1.6 M, 1.6 mmol) in hexane was added by a syringe at -78 °C. The solution was stirred at room temperature for 3 h. Solvent was then removed under vacuum, and the residue was washed with pentane (2 × 6 mL) and recrystallized from the solvent mixture of hexane and ether to give yellow crystals. An NMR tube was flame-dried under vacuum and charged with the title product (47 mg) under argon before it was transferred to a high-vacuum line (10<sup>-6</sup> Torr) trapped with liquid nitrogen. Volatile impurities were pumped out into a liquid nitrogen trap. After 3 h, diethyl ether- $d_{10}$  (0.5 mL) or THF- $d_8$  (0.5 mL) was vacuum transferred to the NMR tube cooled by a liquid nitrogen bath. The cooled NMR tube (N<sub>2</sub> liq) was sealed with a small hot flame.

***cis*- and *trans*-1-D-5-Bis(2-methoxyethyl)-amino-4,4-dimethyl-2-pentene (11cis and 11tr).** Under argon a solution of *n*-butyllithium in hexanes (1.88 mL, 1.6 M, 3 mmol) was added to a solution of amine **8** (688 mg, 3.0 mmol) in diethyl ether at -78 °C. The mixture was allowed to warm to room temperature and stirred for 1 h. Then methanol-OD (495 mg, 15 mmol) was added at -78 °C with stirring, and stirring was continued for 1 h. After the mixture warmed to 0 °C, 8 mL of water was added. The separated aqueous phase was extracted twice with 10 mL of diethyl ether. The

(11) Solomon, S.; Muryr, C. A.; Layfield, R. A. *Chem. Commun.* **2008**, 3142–3144.

(12) (a) Kopecky, K. R.; Levine, C. *Can. J. Chem.* **1981**, 59, 3273–3279. (b) Hart, D. J.; Yang, T. K. *J. Org. Chem.* **1985**, 50, 235–242.

combined organic layer was washed with 10 mL of brine and then dried over MgSO<sub>4</sub>. After removal of volatile components 621 mg of a 1:1 mixture of the title product was obtained in 90% yield. <sup>13</sup>C NMR (CDCl<sub>3</sub>, 62.9 MHz, δ): 14.48, 17.85, 27.17, 27.57, 56.11, 56.24, 58.69, 67.17, 67.64, 71.47, 71.50, 120.49, 122.99. <sup>1</sup>H NMR (CDCl<sub>3</sub>, 250 MHz, δ): 1.106 (s, 6), 1.126 (s, 6), 1.591 (m, 2), 1.663 (m, 2), 2.292 (s, 2), 2.410 (s, 2), 2.68 (m, 8), 3.279 (s, 6), 3.283 (s, 6), 5.2–5.4 (m, 4).

**cis- and trans-5-Bis(2-methoxyethyl)amino-4,4-dimethyl-1-trimethylsilyl-2-propene (12cis and 12tr).** To a solution of **8** (2 g, 8.72 mmol) in 15 mL of diethyl ether, at –78 °C, under an atmosphere of argon, was added a solution of *n*-butyllithium in hexanes (5.63 mL, 1.6 M, 9 mmol). The mixture was slowly warmed to room temperature with stirring and additionally stirred for 2 h. A solution of chlorotrimethylsilane (1.09 g, 10.0 mmol) in 5 mL of diethyl ether was then added at –78 °C with stirring. This mixture was warmed to room temperature and stirred for an additional 3 h, and then 15 mL of water was added at 0 °C. The aqueous phase was extracted twice with 15 mL of diethyl ether each time. The combined organic layer was washed once with 15 mL of brine and then dried over MgSO<sub>4</sub>. After removal of solvent under vacuum there remained 2.6 g of a 1:1 mixture of the title compounds in 95.8% yield. <sup>13</sup>C NMR (CDCl<sub>3</sub>, 62.9 MHz, δ): –1.9, –1.6, 19.9, 22.7, 25.7, 25.9, 38.1, 38.6, 56.2, 58.8, 67.9, 68.2, 71.53, 71.56, 121.9, 124.8, 135.8, 138.1. <sup>1</sup>H NMR (CDCl<sub>3</sub>, 250 MHz, δ): –0.13 (s, 9), –0.08 (s, 9), 0.83 (s, 6), 0.97 (s, 6), 2.22 (s, 2), 2.34 (s, 2), 2.63–2.65 (m, 8), 3.22 (s, 12), 3.32–3.34 (m, 8).

**1-exo,3-exo-5-[Bis(2-methoxyethyl)amino]-4,4-dimethyl-1-trimethylsilyl-2-pentene-1-yl (13ex) and 1-exo,3-endo-5-[Bis(2-methoxyethyl)amino]-4,4-dimethyl-1-trimethylsilyl-2-pentene-1-yl lithium (13).** Under an atmosphere of argon a Schlenk tube was loaded with 4

mL of dry diethyl ether and the 1:1 amine mixture of **12cis** and **12tr** (688 mg, 3 mmol). After the Schlenk tube was cooled to –78 °C, *n*-butyllithium (1.88 mL, 1.6 M, 1.6 mmol) was introduced by a syringe. The resulting mixture was brought to room temperature and stirred for 3 h. Solvent was then removed under vacuum, and the residue was washed with pentane (2 × 6 mL). Then after removal of traces of solvent under vacuum, the remaining solid was recrystallized from a mixture of hexane and diethyl ether. The resulting yellow crystals of the title compounds were pumped dry. A 47 mg portion was transferred into a 5 nm O.D. tube followed by vacuum transfer of 0.5 mL of diethyl ether-*d*<sub>10</sub>. The resulting solution was degassed and then frozen. The sample was then sealed off under vacuum. A second NMR sample was prepared in the same way using THF-*d*<sub>8</sub>. NMR data in text, Figure 3.

**Acknowledgment.** This research was generously supported by the National Science Foundation Grants CHE 0315989 and 0708266 and by the M. S. Newman Chair. We thank Dr. Charles Cottrell, Central Campus Instrumentation Center for untiring technical assistance.

**Supporting Information Available:** Chemical synthesis and NMR data. This material is available free of charge via the Internet at <http://pubs.acs.org>.

JO8022318